Dalton Transactions

Cite this: *Dalton Trans.*, 2011, **40**, 9802

www.rsc.org/dalton

PAPER

Major impact of N-methylation on cytotoxicity and hydrolysis of salan Ti(IV) complexes: sterics and electronics are intertwined†

Sigalit Meker, Cesar M. Manna, Dani Peri and Edit Y. Tshuva*

Received 13th June 2011, Accepted 3rd August 2011
DOI: 10.1039/c1dt11108f

A series of Ti(IV) complexes containing diamino bis(phenolato) "salan" type ligands with NH coordination were prepared, and their hydrolysis and cytotoxicity were analyzed and compared to the N-methylated analogues. Substituting methyl groups on the coordinative nitrogen donor of highly active and stable Ti(IV) salan complexes with H atoms has two main consequences: the hydrolysis rate increases and the cytotoxic activity diminishes. In addition, the small modification of a single replacement of Me with H leads to a different major hydrolysis product, where a dinuclear Ti(IV) complex with two bridging oxo ligands is obtained, as characterized by X-ray crystallography, rather than a trinuclear cluster. A partial hydrolysis product containing a single oxo bridge was also crystallographically analyzed. Investigation of a series of complexes with NH donors of different steric and electronic effects revealed that cytotoxicity may be restored by fine tuning these parameters even for complexes of low stability.

Introduction

Meaningful cytotoxic activities have been reported for complexes of transition metals other than platinum.[1–10] One such metal is Ti(IV), complexes of which, namely titanocene dichloride (Cp_2TiCl_2, Scheme 1a), budotitane ($(bzac)_2Ti(OEt)_2$, Scheme 1b) and their derivatives, have been studied for more than two decades as they possess activity towards cisplatin sensitive and resistant tumor cells with reduced toxicity.[11–19] Their hydrolytic instability and rapid formation of unidentified O-bridged aggregates upon exposure to water, however, impeded their applicability and mechanistic investigations.[13,15,20,21] It therefore is as yet unclear which the cellular target of these compounds is, what the structure of the active species is and what role hydrolysis plays in its formation.

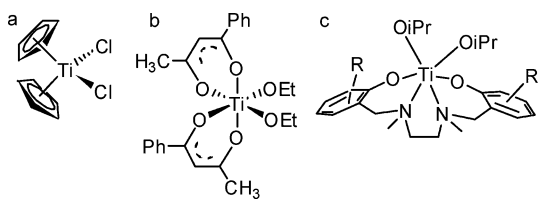

Scheme 1

We have recently developed a new family of C_2-symmetrical Ti(IV) complexes of diamine bis(phenolato) ligands (Scheme 1c), that possess activity towards ovarian OVCAR-1 and colon HT-29 cells that is higher than those of Cp_2TiCl_2, $(bzac)_2Ti(OiPr)_2$ and cisplatin, and their hydrolytic behavior has been investigated.[22–26] It appears that the "salan" type ligands are particularly suitable for stabilizing the active Ti(IV) species where the ligand remains bound for the interaction with the biological target. Thus, we have reported that various complexes with N–Me substitution such as $L^1Ti(OiPr)_2$ (Scheme 2) are highly cytotoxic and highly water-stable, where increasing the N-substituent to Et leads to rapid hydrolysis and no cytotoxicity.[23] Additionally, we observed that steric effects at various locations on the aromatic rings also reduce cytotoxicity, while activity and stability may be enhanced by introducing electronic effects, in particular, with Cl or Br substitutions

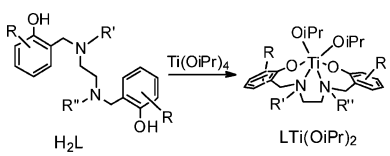

L^1:	R = 3,4-di-Me	R' = R'' = Me
L^2:	R = 3,4-di-Me	R' = Me, R'' = H
L^3:	R = 3,4-di-Me	R' = R'' = H
L^4:	R = 2-Cl	R' = R'' = H
L^5:	R = 2-Cl	R' = R'' = Me
L^6:	R = 2-Br	R' = R'' = H
L^7:	R = 2-Br	R' = R'' = Me
L^8:	R = 2,4-di-Cl	R' = R'' = H
L^9:	R = 2,4-di-Cl	R' = R'' = Me
L^{10}:	R = 4-Me	R' = R'' = H
L^{11}:	R = 4-Me	R' = R'' = Me
L^{12}:	R = H	R' = R'' = H
L^{13}:	R = H	R' = R'' = Me

Scheme 2

Institute of Chemistry, The Hebrew University of Jerusalem, 91904, Jerusalem, Israel. E-mail: tshuva@chem.ch.huji.ac.il; Fax: +972 2 6584282

† CCDC reference numbers 829875–829877. For crystallographic data in CIF or other electronic format see DOI: 10.1039/c1dt11108f

at the *ortho* positions.[22] Considering these findings, and as the well-identified salan-bound trinuclear hydrolysis product lacked cytotoxicity, we proposed that stability is an essential feature, although the involvement of the cluster was also proposed.[22,23] In the current manuscript we report the hydrolytic behavior and cytotoxicity of complexes bearing the NH coordination group in comparison to their *N*-methylated analogues, while analyzing the influence of steric and electronic parameters on the performance of these complexes (Scheme 2).

Results and Discussion

Complexes Synthesis and Characterization

Whereas N-substituted salan ligands such as $H_2L^{1,9,11}$ (Scheme 2) can be easily prepared by a single-step Mannich condensation between the diamine, formaldehyde and the substituted phenol,[22,23] the ligands with secondary amines suffer from their tendency to undergo an additional substitution with formaldehyde to give undesired N–CH_2–N or N–CH_2–O methylene bridges.[27,28] Thus, an alternative stepwise synthesis was employed, involving condensation between the substituted hydroxylbenzaldehyde and the diamine.[29] Additionally, some of the ligands that do not include *para* substitution of the aromatic rings require the stepwise synthetic procedure also for the N-methylated derivatives in order to avoid reaction of formaldehyde at this position.[30] Thus, although H_2L^3 was obtained with high yield by the Mannich condensation, ligands $H_2L^{4,6,8,10,12}$ were prepared by the alternative two-step procedure, where the synthesis of the N-methylated analogues $L^{5,7,13}Ti(OiPr)_2$ was achieved by an additional methylation reaction.[31] H_2L^2 was prepared stepwise from the *N*-methylethylenediamine starting material.

All complexes $L^{1–13}Ti(OiPr)_2$ were synthesized quantitatively as we previously described for $L^1Ti(OiPr)_2$ and analogues,[22,23] from the ligand precursor and $Ti(OiPr)_4$ at RT with THF as the solvent, without addition of a base. The ^{1}H NMR of all complexes except for $L^2Ti(OiPr)_2$ is consistent with C_2-symmetrical structures as obtained for related compounds,[31–34] with *trans* covalent binding of the phenolato groups, two coordinative Ti–NH bonds and *cis* binding of the two isopropoxo ligands, as characterized by a single set of aromatic signals, four doublets of the methylene protons, and a single septet and two doublets of the isopropoxo groups. In contrast, $L^2Ti(OiPr)_2$ is derived from an asymmetric ligand, and thus the complex should exhibit a C_1-symmetry, as is also evident from the eight doublets of the methylene units and four aromatic signals in the ^{1}H NMR. Nevertheless, for this particular complex, the reduced symmetry prevents us determining unequivocally the isomer that is formed, as a *cis*-phenolato compound cannot be ruled out.

Single crystals suitable for X-ray crystallography were grown from a solution of $L^3Ti(OiPr)_2$ in THF. Selected bond lengths and angles are given in Table 1, and an ORTEP drawing of the structure with 50% probability ellipsoids is presented in Fig. 1. The structure is highly similar to those of known complexes of this family,[22,23,31–34] with *trans* phenolato binding and *cis* isopropoxo ligands in accordance with the NMR features. Particularly noteworthy are the Ti–NH distances of 2.26 Å, relative to the 2.34 Å value obtained for $L^1Ti(OiPr)_2$.[24] This shorter bond represents the strong binding of the secondary amine and the reduced steric demands of the H atom, corroborating that a coordinative bond formed without deprotonation. No indications of hydrogen bonding could be detected in the structure.

Table 1 Selected bond lengths (Å) and angles (°) for $L^3Ti(OiPr)_2$

Atoms	Value	Atoms	Value
Lengths			
O(1)–Ti	1.925(3)	N(1)–Ti	2.273(4)
O(2)–Ti	1.917(3)	N(2)–Ti	2.260(4)
O(3)–Ti	1.829(3)	N(1)–H(1 N)	0.75(5)
O(4)–Ti	1.806(3)	N(2)–H(2 N)	0.71(5)
Angles			
O(4)–Ti–O(3)	107.0(2)	O(4)–Ti–N(1)	163.8(2)
O(4)–Ti–O(1)	93.8(1)	O(3)–Ti–N(1)	88.8(2)
O(3)–Ti–O(1)	96.5(1)	O(1)–Ti–N(1)	80.5(1)
O(4)–Ti–O(2)	98.2(1)	O(2)–Ti–N(1)	84.5(1)
O(3)–Ti–O(2)	92.1 (1)	O(4)–Ti–N(2)	90.0(2)
O(1)–Ti–O(2)	162.5 (1)	O(3)–Ti–N(2)	161.9(2)
N(1)–Ti–N(2)	74.7 (1)	O(1)–Ti–N(2)	88.4(1)
		O(2)–Ti–N(2)	79.0(1)

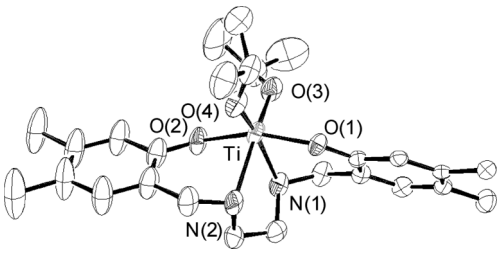

Fig. 1 ORTEP drawing of $L^3Ti(OiPr)_2$ with 50% probability ellipsoids. H atoms were omitted for clarity.

Hydrolysis

Hydrolysis measurements were performed by ^{1}H NMR in 1 : 9 D_2O/THF-d_8 solution as previously described.[22,23] The values obtained for $t_{\frac{1}{2}}$ of the release of the labile isopropoxo ligands are summarized in Table 2. These values are served as a comparative tool between complexes, and do not presume to determine the hydrolysis rate under physiological conditions.

When inspecting Table 2, it is obvious that complexes of NH donors are less stable than their methylated analogues by at least one order of magnitude. In particular, when comparing $L^{1–3}Ti(OiPr)_2$, we observed the additive effect of the elimination

Table 2 $t_{\frac{1}{2}}$ (h) values of isopropoxo release of $L^{1–13}Ti(OiPr)_2$ at 1 : 9 D_2O/THF-d_8 solution at RT

	complex	substitutions	$t_{\frac{1}{2}}$ (h)
parent	$L^1Ti(OiPr)_2$	2,4-di-Me; NMe	5
	$L^2Ti(OiPr)_2$	2,4-di-Me; NMe; NH	0.5
	$L^3Ti(OiPr)_2$	2,4-di-Me; NH	0.2
electronic effects	$L^4Ti(OiPr)_2$	2-Cl; NH	0.5
	$L^5Ti(OiPr)_2$	2-Cl; NMe	50
	$L^6Ti(OiPr)_2$	2-Br; NH	0.5
	$L^7Ti(OiPr)_2$	2-Br; NMe	150
	$L^8Ti(OiPr)_2$	2,4-di-Cl; NH	1
	$L^9Ti(OiPr)_2$	2,4-di-Cl; NMe	110
steric effects	$L^{10}Ti(OiPr)_2$	4-Me; NH	0.2
	$L^{11}Ti(OiPr)_2$	4-Me; NMe	2
	$L^{12}Ti(OiPr)_2$	H; NH	0.2
	$L^{13}Ti(OiPr)_2$	H; NMe	2

of the two N-methyl groups. As we previously observed that larger steric effects on the N-donor substantially decrease the hydrolytic stability,[23] we attribute the effect of the NH groups to electronic reasons. These may relate to hydrogen bonding to water molecules, or to the possibility of deprotonation that may stabilize positive intermediates upon release of anionic labile ligands and therefore accelerate isopropoxo hydrolysis. When examining Table 2, it is apparent that although there are minimal steric effects on the hydrolysis rate, some electronic stabilization occurs for *ortho*-halogenated complexes as observed for the N-methylated analogues;[22] however, the effect is less pronounced, and thus the stability difference for these halogenated complexes between NH and NMe complexes, is up to two orders of magnitude.

We reported previously that the product of the hydrolytic reaction measured for $L^1Ti(OiPr)_2$,[23] as well as other N-methylated complexes of this family,[22] is a highly stable trinuclear compound, where the isopropoxo groups were replaced with water molecules giving oxo bridges, whilst each Ti(IV) center is bound to the salan ligand (Fig. 2). Interestingly, $L^2Ti(OiPr)_2$, differing from $L^1Ti(OiPr)_2$ by a single NH donor replacing an NMe group, yields a different stable hydrolysis product. The X-ray structure of this cluster is provided in Fig. 3 and Selected bond lengths and angles are given in Table 3.

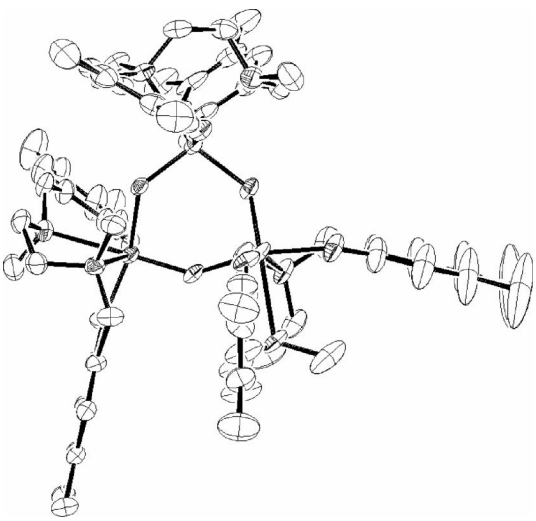

Fig. 2 $L^1{}_3Ti_3(\mu\text{-}O)_3$, hydrolysis product of $L^1Ti(OiPr)_2$.[23]

Table 3 Selected bond lengths (Å) and angles (°) for $L^2{}_2Ti_2(\mu\text{-}O)_2$

Atoms	Value	Atoms	Value
Lengths			
O(1)–Ti	1.7817(14)	N(1)–Ti	2.223(2)
O(2)–Ti	1.9093(15)	N(2)–Ti	2.332(2)
O(3)–Ti	1.8880(16)	N(1)–H(1 N)	0.87(3)
O(1)–Ti	1.9594(15)	Ti . . . Ti	2.8133(7)
Angles			
O(1)–Ti–O(3)	95.42(7)	O(1)–Ti–N(1)	94.87(7)
O(2)–Ti–O(1)	163.12(7)	O(3)–Ti–N(1)	162.33(7)
O(3)–Ti–O(1)	101.82(7)	O(2)–Ti–N(1)	82.50(7)
O(1)–Ti–O(1)	82.59(7)	O(1)–Ti–N(1)	80.91(7)
O(3)–Ti–O(2)	99.48(7)	O(1)–Ti–N(2)	164.37(7)
O(1)–Ti–O(2)	101.93(7)	O(3)–Ti–N(2)	84.92(7)
N(1)–Ti–N(2)	77.48(7)	O(2)–Ti–N(2)	90.68(7)
		O(1)–Ti–N(2)	82.75(6)

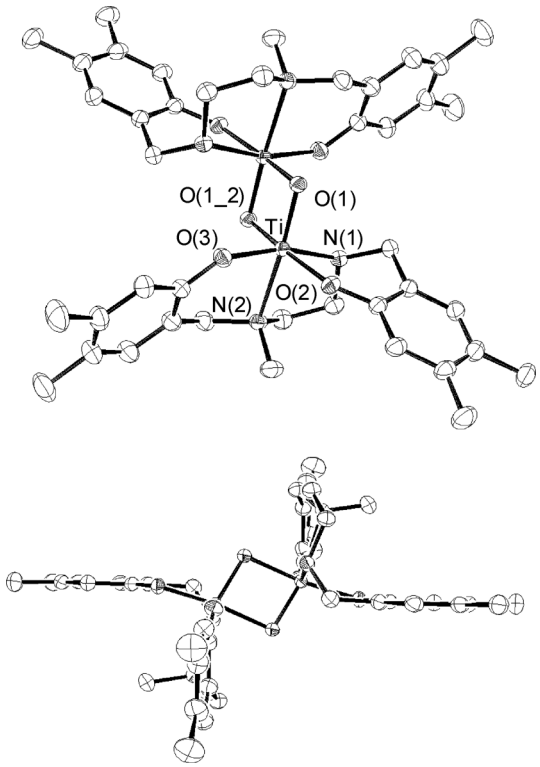

Fig. 3 ORTEP drawing of $L^2{}_2Ti_2(\mu\text{-}O)_2$, the hydrolysis product of $L^2Ti(OiPr)_2$ with 50% probability ellipsoids shown from two angels. H atoms and THF solvent were omitted for clarity.

The structure features a dinuclear complex, with two bridging oxo atoms and a salan ligand bound to each metal center. The two salan ligands bind with a different geometry relative to the starting complex $L^2Ti(OiPr)_2$, with the phenolato oxygen atoms occupying *cis* positions rather than *trans*. This is similar to the observations with different complexes of this type that were obtained following ligand replacement, supporting a similar associative mechanism of this process.[22,23,33] Nevertheless, despite the low C_1-symmetry of the original complex $L^2Ti(OiPr)_2$ resulting from the different N-donors, a center of inversion in the cluster increases its symmetry to C_i. The Ti–O–Ti and O–Ti–O angles of the bridging core are 97.4° and 82.6°, respectively, and the Ti–O–Ti–O moiety is completely planar with a dihedral angle of 180.0°. A short Ti . . . Ti distance of 2.81 Å is observed, and the shortest NH–O distance obtained is 2.4 Å which does not indicate any hydrogen bonding.

Of particular interest is the comparison of the main hydrolysis product of $L^2Ti(OiPr)_2$ (Fig. 2) with that of $L^1Ti(OiPr)_2$ (Fig. 3).[23] Whereas $L^1Ti(OiPr)_2$ yielded a trinuclear complex with a symmetry reduced to C_1 due to two Ti(IV) centers of *cis* phenolato binding and one of a *trans* binding, $L^2Ti(OiPr)_2$ gave rise to a smaller cluster with higher symmetry, despite the relatively small difference between the two precursor isopropoxo complexes that appears to be rather distant from the metal center. Considering that other N-methylated analogues, such as a complex featuring *ortho*-Cl substituents that have significant steric and electronic demands, give rise to similar trinuclear complexes as characterized by X-ray crystallography,[22] we assume that the difference in structure of the hydrolysis product of $L^2Ti(OiPr)_2$ is due to the

Table 4 Selected bond lengths (Å) and angles (°) for $L^4{}_2Ti_2(OiPr)_2(\mu\text{-}O)$

Atoms	Value	Atoms	Value
Lengths			
N(1)–Ti(1)	2.221(2)	O(2)–Ti(1)	1.9285(17)
N(2)–Ti(1)	2.258(2)	O(3)–Ti(1)	1.8895(17)
N(3)–Ti(2)	2.217(2)	O(4)–Ti(1)	1.8588(17)
N(4)–Ti(2)	2.253(2)	O(5)–Ti(2)	1.9272(16)
O(1)–Ti(1)	1.8345(15)	O(6)–Ti(2)	1.8953(17)
O(1)–Ti(2)	1.8406(15)	O(7)–Ti(2)	1.8456(17)
		Ti . . . Ti	3.56
Angles			
Ti(1)–O(1)–Ti(2)	150.91(9)	O(1)–Ti(2)–O(7)	92.46(7)
O(1)–Ti(1)–O(4)	93.37(7)	O(1)–Ti(2)–O(6)	99.30(7)
O(1)–Ti(1)–O(3)	99.47(7)	O(7)–Ti(2)–O(6)	104.89(8)
O(4)–Ti(1)–O(3)	103.87(8)	O(1)–Ti(2)–O(5)	165.56(8)
O(1)–Ti(1)–O(2)	165.79(8)	O(7)–Ti(2)–O(5)	94.37(7)
O(4)–Ti(1)–O(2)	93.13(7)	O(6)–Ti(2)–O(5)	91.23(7)
O(3)–Ti(1)–O(2)	91.21(8)	O(1)–Ti(2)–N(3)	84.36(7)
O(1)–Ti(1)–N(1)	85.14(7)	O(7)–Ti(2)–N(3)	95.32(8)
O(4)–Ti(1)–N(1)	96.52(8)	O(6)–Ti(2)–N(3)	159.22(8)
O(3)–Ti(1)–N(1)	158.73(8)	O(5)–Ti(2)–N(3)	82.35(7)
O(2)–Ti(1)–N(1)	81.58(8)	O(1)–Ti(2)–N(4)	85.38(7)
O(1)–Ti(1)–N(2)	84.66(7)	O(7)–Ti(2)–N(4)	170.51(8)
O(4)–Ti(1)–N(2)	172.08(8)	O(6)–Ti(2)–N(4)	84.59(8)
O(3)–Ti(1)–N(2)	84.04(7)	O(5)–Ti(2)–N(4)	85.80(7)
O(2)–Ti(1)–N(2)	87.18(7)	N(3)–Ti(2)–N(4)	75.29(8)
N(1)–Ti(1)–N(2)	75.68(8)		

electronic properties of the secondary amine coordination site. Additionally, the reduced steric demand of the dinuclear complex (nearest C(*ortho*) . . . C(*ortho*) distance of 7.9 Å) relative to that of the trinuclear cluster (nearest C(*ortho*) . . . C(*ortho*) distance of 3.7 Å) may also account for the increased hydrolysis rate of NH complexes and for the reduced effect of *ortho* substitutions.

Upon exposure to air, $L^4Ti(OiPr)_2$ underwent partial hydrolysis as is obvious from the X-ray structure presented in Fig. 4 (Table 4).[33,35] The structure features a dinuclear cluster, where each Ti(IV) center is bound to the salan ligand and a single oxo ligand bridges the two metal centers, leaving a single isopropoxo group bound to each Ti(IV). In this structure, both phenolato ligands bind in a *cis* configuration as observed for $L^2{}_2Ti_2(\mu\text{-}O)_2$ and related structures of such LigTiOR–O–TiORLig (Lig: salan ligand) moiety,[33] supporting the main ligand rearrangement occurring upon the first ligand replacement interaction. The symmetry of the structure is reduced to C_1 by the bend of the single oxo bridge, and the Ti . . . Ti distance is 3.56 Å.

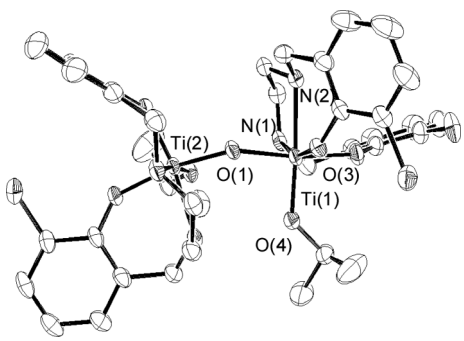

Fig. 4 ORTEP drawing of $L^4{}_2Ti_2(OiPr)_2(\mu\text{-}O)$, the partial hydrolysis product of $L^4Ti(OiPr)_2$ with 50% probability ellipsoids. H atoms and ether solvent were omitted for clarity.

Table 5 Absolute IC_{50} (μM) values of $L^{1\text{–}13}Ti(OiPr)_2$ and reference compounds towards colon HT-29 and ovarian OVCAR-1 cells

	complex	substitutions	HT-29 (μM)	OVCAR-1 (μM)
parent	$L^1Ti(OiPr)_2$	2,4-di-Me; NMe	10 ± 1	10 ± 1
	$L^2Ti(OiPr)_2$	2,4-di-Me; NMe; NH	—[a]	—[a]
	$L^3Ti(OiPr)_2$	2,4-di-Me; NH	—[a]	—[a]
electronic	$L^4Ti(OiPr)_2$	2-Cl; NH	21 ± 1	43 ± 1
effects	$L^5Ti(OiPr)_2$	2-Cl; NMe	4 ± 1	8 ± 1
	$L^6Ti(OiPr)_2$	2-Br; NH	50 ± 1	98 ± 2
	$L^7Ti(OiPr)_2$	2-Br; NMe	12 ± 1	0.9 ± 1.1
	$L^8Ti(OiPr)_2$	2,4-di-Cl; NH	—[a]	—[a]
	$L^9Ti(OiPr)_2$	2,4-di-Cl; NMe	—[a]	—[a]
steric effects	$L^{10}Ti(OiPr)_2$	4-Me; NH	15 ± 1	7 ± 1
	$L^{11}Ti(OiPr)_2$	4-Me; NMe	7 ± 1	7 ± 1
	$L^{12}Ti(OiPr)_2$	H; NH	14 ± 1	36 ± 1
	$L^{13}Ti(OiPr)_2$	H; NMe	17 ± 1	20 ± 1
reference	Cp_2TiCl_2		641 ± 1	741 ± 1
	$(bzac)_2Ti(OiPr)_2$		17 ± 1	17 ± 1
	cisplatin		12 ± 1	10 ± 1

[a] Growth inhibition does not reach 50%.

Cytotoxicity

Cytotoxicity was measured on ovarian OVCAR-1 and colon HT-29 cells based on the MTT assay following a three day incubation period as previously described.[22] The IC_{50} values are summarized in Table 5.

When inspecting the results for complexes $L^{1\text{–}3}Ti(OiPr)_2$ it appears that, as we previously reported,[22,23] the cytotoxic activity is related to the hydrolytic stability (Fig. 5). Thus, increasing the number of NH relative to NMe donors which decreases not only the hydrolytic stability but the cytotoxicity as well. Complex $L^3Ti(OiPr)_2$ is practically inactive, while $L^2Ti(OiPr)_2$ demonstrates a mild activity. Additionally, the dimeric hydrolysis product $L^2{}_2Ti_2(\mu\text{-}O)_2$ is also completely inactive, further supporting the notion that the stability of the precursor complexes is of importance for cytotoxicity.

Complexes $L^{4\text{–}13}Ti(OiPr)_2$ were analyzed in an attempt to elucidate the relations between the parameters affecting cytotoxicity, where steric and electronic effects known to enhance activity in the N-methylated complexes were introduced to complexes of NH donors.

As for electronic effects, the *ortho* chlorinated and *ortho* brominated complexes of NH donors $L^{4,6}Ti(OiPr)_2$ showed somewhat enhanced cytotoxicity relative to the corresponsing non-halogenated complexes[22] (Fig. 6, Table 5), although their activity is still markedly lower than those of the N-methylated analogues, for which the halogenation effect is more pronounced giving particularly active complexes. When inspecting the hydrolysis rates, it might appear as though the increased stability might be the reason for the enhanced activity, although the stability enhancement for the *ortho* halogenated NH complexes is relatively minor. Additionally, complex $L^8Ti(OiPr)_2$ of the highest stability of this series demonstrated the lowest cytotoxicity, implying that the relationship between these structural parameters is more complex, where steric effects might play a particularly meaningful role.[23] Thus, sterics may account both for the reduced activity of the *ortho*, *para* dichlorinated complex $L^8Ti(OiPr)_2$ and for the reduced activity of the *ortho* brominated complex $L^6Ti(OiPr)_2$ relative to the *ortho* chlorinated one $L^4Ti(OiPr)_2$, a pattern

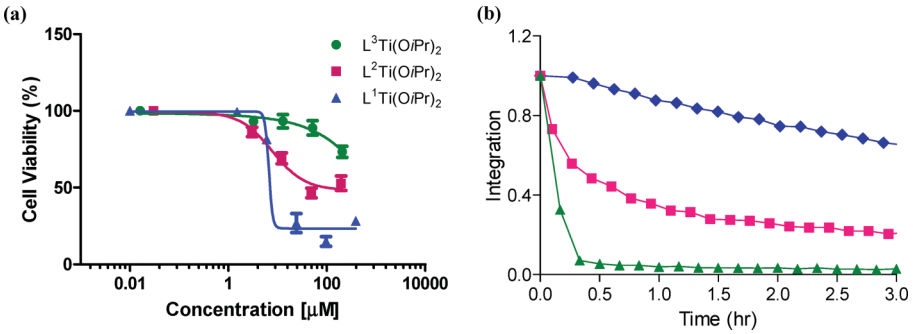

Fig. 5 Dependence of HT-29 cell viability after a 3 day incubation period on administered concentration of $L^{1-3}Ti(OiPr)_2$ (a) and plot of integration of bound isopropoxo signals in the ^1H NMR of $L^{1-3}Ti(OiPr)_2$ vs. time following addition of D_2O to the THF-d_8 solution at RT (b).

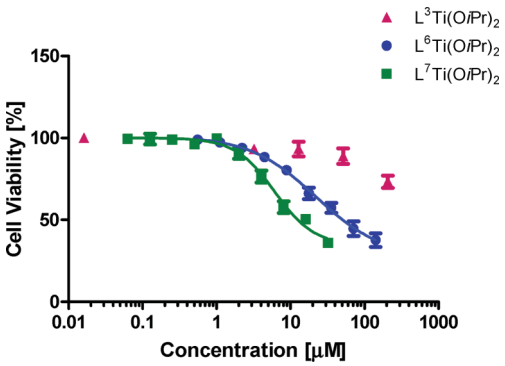

Fig. 6 Dependence of HT-29 cell viability after a 3 day incubation period on administered concentration of $L^{3,6,7}Ti(OiPr)_2$.

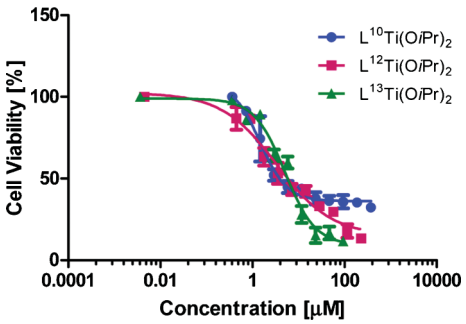

Fig. 7 Dependence of HT-29 cell viability after a 3 day incubation period on administered concentration of $L^{10,12,13}Ti(OiPr)_2$.

somewhat different than that observed for the N-methylated analogues.[22] It thus appears that steric effects are more pronounced for complexes of NH donors, which urged us to further analyze such effects for this series of complexes.

Analyzing steric effects included eliminating first one ($L^{10}Ti(OiPr)_2$) and then both ($L^{12}Ti(OiPr)_2$) of the two methyl substitutions in each aromatic ring of $L^3Ti(OiPr)_2$, and comparing the performance of the complexes to those of the N-methylated analogues ($L^{11,13}Ti(OiPr)_2$ respectively). A major effect of steric crowding is demonstrated, where the activity of the NH complexes could be almost completely restored by eliminating the aromatic methyl substitutions, despite their relatively rapid hydrolysis (Fig. 7). Thus, the activities of $L^{10}Ti(OiPr)_2$ and $L^{12}Ti(OiPr)_2$, which are substantially higher than that of $L^3Ti(OiPr)_2$, are mostly similar to that of $L^{13}Ti(OiPr)_2$, while no marked improvement is observed for $L^{11,13}Ti(OiPr)_2$ relative to $L^1Ti(OiPr)_2$. It may therefore be concluded that steric effects are more meaningful for complexes of NH donors, in spite, or perhaps because of their reduced hydrolytic stability.

Conclusion

In this paper we have compared a new series of salan Ti(IV) complexes of NH donors to their N-methylated analogues. Whereas marked stability and cytotoxicity enhancement is observed for N-methylated complexes upon *ortho* halogenation, giving particularly active complexes with activity that mostly exceeds that of cisplatin, this effect is relatively minor for complexes of NH donors. In contrast, the elimination of steric groups is particularly efficient in enhancing the cytotoxic activity of complexes of NH donors, giving complexes of activity similar to that of the corresponding N-methylated compounds and higher activity than that of their *ortho* halogenated NH analogues. Of particular interest is the observation that complexes resulting from relatively rapid hydrolysis may be highly cytotoxic if steric effects are eliminated. It is therefore tempting to argue that rapidly hydrolyzed complexes are more sensitive to structural modifications of a steric nature, as these complexes may encounter kinetic obstacles that are size dependent, and thus stable complexes, even if bulky, may overcome them. Such obstacles may relate to cell penetration, interaction with macromolecules *via* transport and reactivity, *etc*.

Another interesting point, when comparing complexes of NH donors to the N-methylated ones, relates to the different hydrolysis products. Whereas N-methylated complexes of different aromatic substituents give trinuclear oxo-bridged clusters as the major hydrolysis products,[22,23] complexes of NH donors give dimeric structures,[36] which are higher in symmetry and smaller in size. This may account for some of the differences observed in the behavior of these complexes, since we have previously noticed a correlation between the ability of a complex to form such salan-bound clusters upon hydrolysis and its ability to induce cytotoxic effects, suggesting involvement of the cluster in the activity.[23] Nevertheless, both clusters were found to be inactive, raising the possibility that a steric obstacle might relate to cell penetration where their activity may possibly be pronounced if they are formed in the cellular environment only (Scheme 3). Therefore, smaller clusters of reduced steric demands may both account for the increased hydrolysis rate and for the diminished dependence on it. We are currently promoting this line of research in an attempt

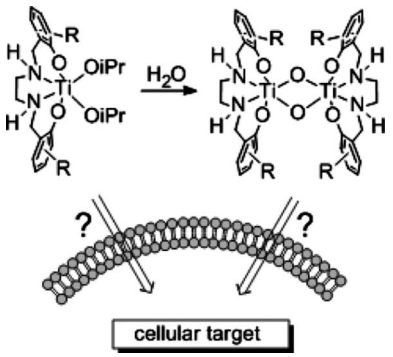

Scheme 3

to elucidate the active inner-cellular species, its penetration mode, and its target.

Experimental Section

Ligands H_2L[1,9–13] and Ti(IV) complexes $L^{1,9,11-13}Ti(OiPr)_2$ were synthesized as previously described.[21,22,24,29,30] Paraformaldehyde (~95%), formaldehyde (37–41% in water), *N*,*N*′-dimethylethylenediamine (99%), *N*-methylethylenediamine (95%), ethylenediamine (98%) and all substituted phenol compounds (>97%) were purchased from Aldrich Chemical Company Inc., Across Organics or Fluka Riedel-deHaen. Titanium tetra(isopropoxide) (97%) was purchased from Aldrich Chemical Company Inc. All solvents were distilled from K or K/benzophenone under nitrogen, or dried over an aluminum column on an M. Braun drying system SPS-800. All experiments requiring a dry atmosphere were performed in an M. Braun dry-box or under a nitrogen atmosphere using Schlenck line techniques. NMR data were recorded using AMX-400 MHz or AMX-500 MHz Bruker spectrometers. X-Ray diffraction data were obtained with a Bruker SMART APEX CCD diffractometer, running the SMART software package. After collection, the raw data frames were integrated by the SAINT software package. The structures were solved and refined using the SHELXTL software package. Elemental analyses were performed in the microanalytical laboratory in our institute. Accurare-Mass QTOF LC/MS measurements were carried on an Agilent Technologies 6520 instrument. Cytotoxicity was measured on HT-29 colon and OVCAR-1 ovarian cells obtained from ATCC Inc. using the methylthiazolyldiphenyl-tetrazolium bromide (MTT) assay as previously described.[22] Absolute IC_{50} values were determined by a non-linear regression of a variable slope (four parameters) model. Kinetic studies by NMR were performed as previously described, using 6 mM of the complex solution in THF-d_8 and adding >1000 equiv. of D_2O to give a final solution of 1 : 9 D_2O/THF-d_8. The $t_{\frac{1}{2}}$ value is based on a pseudo first order fit for each compound. The results were verified by including *p*-dinitrobenzene as an internal standard.

H_2L^2 was synthesized by refluxing 3,4-dimethylphenol (2.44 g, 20.0 mmol) with paraformaldehyde (0.60 g, 20.0 mmol) and *N*-methylethylenediamine (0.3 ml, 10.0 mmol) in methylene chloride for 4 h. The solvent was removed by vacuum and the crude product was dissolved in methanol : hexane 5 : 1 solution, which was allowed to cool to –4 °C overnight. The colorless precipitate was filtered and washed with cold methanol to yield **H_2L^2** (0.7 g, 20%). ^{1}H NMR (400 MHz, $CDCl_3$): δ 6.71 (1 H, s, Ar), 6.69 (1 H, s, Ar), 6.63 (1 H, s, Ar), 6.57 (1 H, s, Ar), 3.93 (2 H, s, CH_2), 3.64 (2 H, s, CH_2), 2.95 (2 H, t, J = 6.4 Hz, CH_2), 2.65 (2 H, t, J = 6.4 Hz, CH_2), 2.28 (3 H, s, CH_3), 2.19 (3 H, s, CH_3), 2.18, (3 H, s, CH_3), 2.16 ppm (6 H, s, CH_3); ^{13}C NMR (100 MHz, $CDCl_3$): δ 155.3, 151.8, 136.2, 130.3, 128.7, 128.3, 127.1, 117.9, 117.3, 116.8, 82.4, 77.2, 59.7, 54.4, 49.9, 48.0, 41.2, 19.6, 19.5, 18.8, 18.7 ppm; Found: C, 73.61; H, 8.37; N, 7.63. Calc. for $C_{21}H_{30}N_2O_2$: C, 73.65; H, 8.83; N, 8.18%.

H_2L^3 was prepared by refluxing 3,4-dimethylphenol (3.67 g, 30 mmol), paraformaldehyde (0.30 g, 10 mmol), and ethylenediamine (0.3 ml, 5 mmol) in methanol for 5 h. The solution was cooled to –4 °C, and a colorless solid precipitated. The precipitate was filtered and washed with methanol to yield **H_2L^3** (0.9 g, 55%). ^{1}H NMR (500 MHz, $CDCl_3$): δ 6.72 (2 H, s, Ar), 6.64 (2 H, s, Ar), 3.93 (4 H, s, CH_2), 2.82 (4 H, s, CH_2), 2.19 (6 H, s, CH_3), 2.17 ppm (6 H, s, CH_3); ^{13}C NMR (125 MHz, $CDCl_3$): δ 155.9, 137.2, 129.6, 127.0, 119.4, 117.8, 52.4, 48.0, 19.7 ppm; Found: C, 73.11; H, 8.57; N, 8.40. Calc. for $C_{20}H_{28}N_2O_2$: C, 73.14; H, 8.59; N, 8.53%.

H_2L^4 was synthesized by slowly adding to a stirred solution of 3-chloro-2-hydroxybenzaldehyde (1.57 gr, 10 mmol) in 10 ml of methanol a solution of ethylenediamine (0.3 ml, 5 mmol) in 30 ml methanol. The solution was stirred for 3 h at RT during which a color change to yellow was observed. $NaBH_4$ (1.51 g, 40 mmol) was added in small portions, and the reaction was stirred overnight. The solution became colorless and a colorless solid precipitated. 100 ml of water were added, and the precipitate was collected by vacuum filtration to yield **H_2L^4** (0.4 g, 45%). ^{1}H NMR (500 MHz, $CDCl_3$): δ 7.26 (2 H, d, J = 7.6 Hz, Ar), 6.89 (2 H, d, J = 7.4 Hz, Ar), 6.73 (2 H, t, J = 7.6 Hz, Ar) 4.01 (4 H, s, CH_2), 2.85 ppm (4 H, s, CH_2); ^{13}C NMR (125 MHz, $CDCl_3$): δ 153.9, 129.5, 127.0, 123.6, 121.4, 119.8, 52.6, 47.9 ppm; Found: C, 56.10; H, 5.27; N, 7.89. Calc. for $C_{16}H_{18}Cl_2N_2O_2$: C, 56.32; H, 5.32; N, 8.21%.

H_2L^5 was synthesized by dissolving **H_2L^4** (0.98 g, 2.9 mmol) in acetonitrile (110 ml) and acetic acid (15 ml). Formaldehyde was added (5.5 ml, 70 mmol, 37–41% in water), and the mixture was stirred for 45 min. $NaBH_4$ was added (1.51 g, 40 mmol) and the reaction was stirred for 12 h. The solvent was removed *in vacuo*. The residue was hydrolyzed with 50 ml 2 M NaOH, leading to precipitation of a colorless solid. The precipitate was collected by vacuum filtration and was washed with methanol to yield **H_2L^5** (0.8 g, 78%). ^{1}H NMR (500 MHz, THF-d_8): δ 7.19 (2 H, d, J = 8.0 Hz, Ar), 6.93 (2 H, d, J = 7.5 Hz, Ar), 6.67 (2 H, t, J = 8.0 Hz, Ar), 3.74 (4 H, s, CH_2), 2.71 (4 H, s, CH_2), 2.28 (6 H, s, CH_3); ^{13}C NMR (125 MHz, THF-d_8): δ 155.1, 130.0, 128.1, 125.0, 121.8, 120.0, 61.7, 55.0, 41.9 ppm; Found: C, 58.25; H, 5.81; N, 7.53. Calc. for $C_{18}H_{22}Cl_2N_2O_2$: C, 58.54; H, 6.00; N, 7.59%.

H_2L^6 was synthesized by slowly adding to a stirred solution of 3-bromo-2-hydroxybenzaldehyde (2.00 g, 10 mmol) in 10 ml of methanol a solution of ethylenediamine (0.35 ml, 5.0 mmol) in 30 ml methanol. The solution was stirred for 10 h at RT during which a color change to yellow was observed. $NaBH_4$ (1.51 g, 40 mmol) was added in small portions, and the reaction was stirred overnight. The solution became colorless and a colorless solid precipitated. 100 ml of water was added, and the precipitate was collected by vacuum filtration to yield **H_2L^6** (0.6 g, 30%). ^{1}H NMR (500 MHz, THF-d_8): δ 7.43 (2 H, d, J = 8.0 Hz, Ar), 6.94 (2 H, d, J = 7.5 Hz, Ar), 6.68 (2 H, t, J = 8.0 Hz, Ar), 4.00 (4 H, s, CH_2), 2.85 ppm (4 H, s, CH_2); ^{13}C NMR (125 MHz, THF-d_8): δ 154.8,

132.5, 127.8, 123.5, 120.4, 110.7, 52.7, 47.9 ppm; Found: C, 44.14; H, 4.15; N, 6.13. Calc. for $C_{16}H_{18}Br_2N_2O_2$: C, 44.68; H, 4.22; N, 6.51%.

H_2L^7 was synthesized by dissolving **H_2L^6** (0.64 g, 1.5 mmol) in acetonitrile (110 ml) and acetic acid (15 ml). Formaldehyde was added (5.5 ml, 70 mmol, 37–41% in water), and the mixture was stirred for 10 min. $NaBH_4$ was added (1.51 g, 40 mmol) and the reaction was stirred for 12 h. The solvent was removed *in vacuo*. The residue was hydrolyzed with 50 ml 2 M NaOH, leading to precipitation of a white solid. The precipitate was collected by vacuum filtration and was washed with methanol to yield **H_2L^7** (0.4 g, 60%). ^{1}H NMR (500 MHz, THF-d_8): δ 7.36 (2 H, dd, J = 6.5, 1.5 Hz, Ar), 6.96 (2 H, dd, J = 6.0, 1.5 Hz, Ar), 6.62 (2 H, t, J = 8.0 Hz, Ar), 3.74(4 H, s, CH_2), 2.72 ppm (4 H, s, CH_2), 2.28 ppm (6 H, s, CH_3); ^{13}C NMR (125 MHz, THF-d_8): δ 156.2, 133.0, 128.8, 124.8, 120.6, 111.0, 62.0, 54.9, 41.9 ppm; Found: C, 46.88; H, 4.62; N, 5.81. Calc. for $C_{18}H_{22}Br_2N_2O_2$: C, 47.18; H, 4.84; N, 6.11%.

H_2L^8 was synthesized by adding to a stirred solution of 3,5-dichloro-2-hydroxybenzaldehyde (1.91 g, 10 mmol) in 10 ml of methanol a solution of ethylenediamine (0.3 ml, 5 mmol) in 30 ml methanol. The solution was stirred for 15 min at RT during which a color change to yellow was observed. $NaBH_4$ (1.51 g, 40 mmol) was added in small portions, and the reaction was stirred overnight. The solution became colorless and a colorless solid precipitated. 200 ml of water was added, and the precipitate was collected by vacuum filtration to yield **H_2L^8** (0.8 g, 40%). ^{1}H NMR (500 MHz, THF-d_8): δ 7.23 (2 H, d, J = 3.5 Hz, Ar), 6.99 (2 H, dt, J = 1.0, 2.5 Hz, Ar), 3.96 (4 H, s, CH_2), 2.78 ppm (4 H, s, CH_2); ^{13}C NMR (125 MHz, THF-d_8): δ 153.4, 127.8, 126.5, 126.0, 122.5, 121.2, 51.4, 47.4 ppm; Found: C, 46.93; H, 3.88; N, 6.77. Calc. for $C_{16}H_{16}Cl_4N_2O_2$: C, 46.86; H, 3.93; N, 6.83%.

$L^{2\text{–}8,10}$Ti(O*i*Pr)$_2$ were synthesized as previously described by reacting **$H_2L^{2\text{–}8,10}$** (0.2 mmol) with Ti(O*i*Pr)$_4$ (0.05 g, 0.2 mmol) in dry THF at RT for 2 h. Following removal of the solvent, the products were obtained as yellow solids in quantitative yields.

L^2Ti(O*i*Pr)$_2$

^{1}H NMR (500 MHz, $CDCl_3$): δ 6.75 (1 H, s, Ar), 6.67 (1 H, s, Ar), 6.49 (1 H, s, Ar), 6.48 (1 H, s, Ar) 4.99 (1 H, sept, J = 6.0 Hz, C*H*CH_3), 4.95 (1 H, sept, J = 6.0 Hz, C*H*CH_3), 4.54 (1 H, d, J = 13.2 Hz, CH_2), 4.27 (1 H, d, J = 13.2 Hz, CH_2), 3.83 (1 H, d, J = 13.6 Hz, CH_2), 3.02 (1 H, d, J = 13.6 Hz, CH_2), 2.91 (1 H, dt, J = 13.2, 3.6 Hz, CH_2), 2.64 (1 H, dt, J = 13.2, 3.6 Hz, CH_2), 2.52 (1 H, dt, J = 13.2, 2.5 Hz, CH_2), 2.48 (3 H, s, CH_3), 2.20–2.10 (12 H, m, CH_3), 1.70 (1 H, dt, J = 13.2, 3.0 Hz, CH_2), 1.28–1.17 ppm (12 H, m, CHC*H*$_3$); ^{13}C NMR (100 MHz, $CDCl_3$): δ160.0, 159.8, 467.0, 136.9, 131.0, 130.4, 125.3, 125.2, 122.1, 121.8, 118.5, 118.4, 77.9, 71.6, 64.2, 56.3, 51.9, 47.6, 43.4, 26.0, 25.8, 22.2, 22.1, 19.6 ppm; HRMS ($C_{27}H_{42}N_2O_4Ti$ +H) Calc: 507.2702 Found: 507.2697.

L^3Ti(O*i*Pr)$_2$

^{1}H NMR (500 MHz, $CDCl_3$): δ 6.68 (2 H, s, Ar), 6.51 (2 H, s, Ar), 4.90 (2 H, sept, J = 6.1 Hz, C*H*CH_3), 4.62 (2 H, d, J = 13.0 Hz, CH_2), 4.48 (2 H, d, J = 13.0 Hz, CH_2), 2.90 (2 H, s, NH), 2.56 (2 H, m, CH_2), 2.49 (2 H, m, CH_2), 2.17 (6 H, s, CH_3), 2.13 (6 H, s, CH_3), 1.26 (6 H, d, J = 6.1 Hz, CHC*H*$_3$), 1.23 ppm (6 H, d, J = 6.0 Hz, CHC*H*$_3$); ^{13}C NMR (125 MHz, $CDCl_3$): δ 160.9, 137.0, 130.4, 125.2, 120.9, 118.9, 77.1, 53.3, 48.3, 26.0, 25.9, 19.7, 18.8 ppm; HRMS ($C_{26}H_{40}N_2O_4Ti$ +H) Calc: 493.2546 Found: 493.2543. Single crystals of **L^3Ti(O*i*Pr)$_2$** were obtained from a solution of hexane at –35 °C.

Crystal data for L^3Ti(O*i*Pr)$_2$

$C_{26}H_{40}N_2O_4Ti$, M = 492.50, Trigonal, a,b = 19.5096(9) Å, c = 12.402(1) Å, V = 4088.1(5) Å^3, T = 173(2) K, space group $P\bar{3}$, Z = 6, μ($Mo_{K\alpha}$) = 0.345 mm^{-1}, 42199 reflections measured, 5370 unique (R_{int} = 0.0365), R(F°^{2}) for [$I > 2\sigma(I)$] = 0.0973, Rw for [$I > 2\sigma(I)$] = 0.2425.

L^4Ti(O*i*Pr)$_2$

^{1}H NMR (500 MHz, THF-d_8): δ 7.15 (2 H, d, J = 7.5 Hz, Ar), 6.85 (2 H, d, J = 7.5 Hz, Ar), 6.51 (2 H, t, J = 7.5 Hz, Ar), 5.11 (2 H, sept, J = 6.0 Hz, C*H*CH_3), 4.75 (2 H, d, J = 12.0 Hz, CH_2), 3.88 (2 H, s, NH), 3.73 (2 H, d, J = 14.0 Hz, CH_2), 2.59 (2 H, m, CH_2), 2.50 (2 H, m, CH_2), 1.24 (6 H, d, J = 6.0 Hz, CHC*H*$_3$), 1.20 ppm (6 H, d, J = 6.0 Hz, CHC*H*$_3$); ^{13}C NMR (125 MHz, THF-d_8): 159.1, 129.5, 128.6, 125.9, 123.2, 117.6, 78.2, 54.2, 47.8, 26.5, 26.4 ppm; HRMS ($C_{22}H_{30}Cl_2N_2O_4Ti$ +H) Calc: 505.1140 Found: 505.1138

L^5Ti(O*i*Pr)$_2$

^{1}H NMR (500 MHz, THF-d_8): δ 7.23 (2 H, dd, J = 8.0, 2.6 Hz, Ar), 6.90 (2 H, d, J = 7.0 Hz, Ar), 6.57 (2 H, t, J = 8.0 Hz, Ar), 5.26 (2 H, sept, J = 6.0 Hz, C*H*CH_3), 4.67 (2 H, d, J = 13.5 Hz, CH_2), 3.28 (2 H, d, J = 13.5 Hz, CH_2), 2.94 (2 H, d, J = 9.5, Hz, CH_2), 2.48 (6 H, s, CH_3), 1.91 (2 H, d, J = 9.5 Hz, CH_2), 1.30 (6 H, d, J = 6.0 Hz, CHC*H*$_3$), 1.22 ppm (6 H, d, J = 6.0 Hz, CHC*H*$_3$); ^{13}C NMR (125 MHz, THF-d_8): δ 158.7, 130.3, 129.0, 127.1, 122.7, 118.3, 79.2, 65.1, 52.7, 47.7, 26.8, 26.3 ppm; Anal. Calc. for $C_{24}H_{34}Cl_2N_2O_4Ti$: C, 54.05; H, 6.43; N, 5.25; found: C, 54.05; H, 6.26; N, 5.33.

L^6Ti(O*i*Pr)$_2$

^{1}H NMR (500 MHz, THF-d_8): δ 7.34 (2 H, d, J = 7.5 Hz, Ar), 6.89 (2 H, d, J = 7.5 Hz, Ar), 6.45 (2 H, t, J = 7.5 Hz, Ar), 5.17 (2 H, sept, J = 6.0 Hz, C*H*CH_3), 4.76 (2 H, d, J = 12.4 Hz, CH_2), 3.84 (2 H, s, NH), 3.66 (2 H, d, J = 14.0 Hz, CH_2), 2.60 (2 H, m, CH_2), 2.52 (2 H, m, CH_2), 1.24 (6 H, d, J = 6.0 Hz, CHC*H*$_3$), 1.20 ppm (6 H, d, J = 6.0 Hz, CHC*H*$_3$); ^{13}C NMR (100 MHz, THF-d_8): 160.0, 132.7, 129.4, 125.9, 118.2, 113.8, 78.2, 54.3, 47.8, 26.6, 26.5 ppm; HRMS ($C_{22}H_{30}Br_2N_2O_4Ti$ + Na) Calc: 616.9929 Found: 616.9924.

L^7Ti(O*i*Pr)$_2$

^{1}H NMR (500 MHz, THF-d_8): δ 7.39 (2 H, d, J = 8.0, Hz, Ar), 6.93 (2 H, d, J = 7.5 Hz, Ar), 6.52 (2 H, t, J = 7.5 Hz, Ar), 5.32 (2 H, sept, J = 6.0 Hz, C*H*CH_3), 4.67 (2 H, d, J = 13.5 Hz, CH_2), 3.26 (2 H, d, J = 13.5 Hz, CH_2), 2.94 (2 H, d, J = 9.5, Hz, CH_2), 2.49 (6 H, s, CH_3), 1.89 (2 H, d, J = 9.5 Hz, CH_2), 1.30 (6 H, d, J = 6.0 Hz, CHC*H*$_3$), 1.22 ppm (6 H, d, J = 6.0 Hz, CHC*H*$_3$); ^{13}C NMR (100 MHz, $CDCl_3$): δ 158.3, 132.6, 128.7, 125.5, 118.0, 112.4, 78.8, 64.5, 51.6, 47.4, 26.1, 25.7 ppm; Anal. Calc. for $C_{24}H_{34}Br_2N_2O_4Ti$: C, 46.33; H, 5.51; N, 4.50; Found: C, 45.97; H, 5.22; N, 4.20.

$L^8Ti(OiPr)_2$

^{1}H NMR (400 MHz, $CDCl_3$): δ 7.25 (2 H, s, Ar), 6.86 (2 H, s, Ar), 4.99 (2 H, sept, J = 6.1 Hz, C*H*CH$_3$), 4.71 (2 H, d, J = 13.8 Hz, CH_2), 3.61 (2 H, d, J = 13.8 Hz, CH_2), 2.92 (2 H, s, NH), 2.64 (2 H, m, CH_2), 2.52 (2 H, m, CH_2), 1.26 (6 H, d, J = 6.1 Hz, CHC*H*$_3$), 1.23 ppm (6 H, d, J = 6.0 Hz, CHC*H*$_3$); ^{13}C NMR (100 MHz, $CDCl_3$): 157.1, 128.9, 127.6, 125.2, 123.2, 121.1, 78.9, 53.2, 47.5, 25.7, 25.6 ppm; HRMS ($C_{22}H_{28}Cl_4N_2O_4Ti$ +H) Calc: 575.0332 Found: 575.0331.

$L^{10}Ti(OiPr)_2$

^{1}H NMR (500 MHz, THF-d_8): δ 6.80 (2 H, d, J = 8.0 Hz, Ar), 6.70 (2 H, s, Ar), 6.40 (2 H, d, J = 8.0 Hz, Ar), 4.86 (2 H, sept, J = 6.0 Hz, C*H*CH$_3$), 4.62 (2 H, d, J = 13.5 Hz, CH_2), 3.80 (2 H, s, NH), 3.50 (2 H, d, J = 12.5 Hz, CH_2), 2.49 (4 H, m, CH_2), 2.14 (6 H, s, CH_3) 1.17 (6 H, d, J = 6.0 Hz, CHC*H*$_3$), 1.17 ppm (6 H, d, J = 6.0 Hz, CHC*H*$_3$); ^{13}C NMR (125 MHz, THF-d_8): 161.8, 130.4, 129.5, 126.1, 124.3, 118.2, 77.3, 76.9, 54.3, 48.3, 26.6, 20.9 ppm; HRMS ($C_{24}H_{36}N_2O_4Ti$ +H) Calc: 465.2233 Found: 465.2230.

Crystal data for $L^2{}_2Ti_2(\mu\text{-}O)_2$

$C_{42}H_{56}N_4O_6Ti_2{\cdot}C_4H_8O$ (the structure contains a single THF solvent molecule), M = 880.81, triclinic, a = 6.983(1), b = 12.706(2), c = 14.613(2) Å, α = 66.685(2)°, β = 84.776(3)°, γ = 83.530(3)°, V = 1181.4(3) Å^3, T = 293(2) K, space group $P\bar{1}$, Z = 1, $\mu(Mo_{K\alpha})$ = 0.389 mm^{-1}, 13613 reflections measured, 5470 unique (R_{int} = 0.0193), $R(F^{\circ 2})$ for $[I > 2\sigma(I)]$ = 0.0507, Rw for $[I > 2\sigma(I)]$ = 0.1548.

Crystal data for $L^4{}_2Ti_2(OiPr)_2(\mu\text{-}O)$

$C_{38}H_{45}Cl_4N_4O_7Ti_2{\cdot}0.5(C_4H_{10}O)$ (the structure contains 0.5 diethylether solvent molecule), M = 944.44, Monoclinic, a = 13.059(1) Å, b = 23.948(2) Å, c = 15.351(2) Å, β = 95.966(2)°, V = 4774.8(8) Å^3, T = 173(1) K, space group $P2_1/c$, Z = 4, $\mu(Mo_{K\alpha})$ = 0.607 mm^{-1}, 51349 reflections measured, 10419 unique (R_{int} = 0.0316), $R(F^{\circ 2})$ for $[I > 2\sigma(I)]$ = 0.0555, Rw for $[I > 2\sigma(I)]$ = 0.1667.

Supporting information available

Crystallographic data for $L^3Ti(OiPr)_2$, $L^2{}_2Ti_2(\mu\text{-}O)_2$ and $L^4{}_2Ti_2(OiPr)_2(\mu\text{-}O)$.†

Acknowledgements

We thank Dr Shmuel Cohen for solution of the X-ray structures. This research received funding from the European Research Council under the European Community's Seventh Framework Programme (FP7/2007-2013)/ERC Grant agreement n° [239603]. The research was also partly supported the Israel Science Foundation (grant No.124/09) and the Lower Saxony Ministry of Science.

References

1 P. C. A. Bruijnincx and P. J. Sadler, *Curr. Opin. Chem. Biol.*, 2008, **12**, 197–206.
2 M. J. Clarke, F. Zhu and D. R. Frasca, *Chem. Rev.*, 1999, **99**, 2511–2543.
3 B. Desoize, *Anticancer Res.*, 2004, **24**, 1529–1544.
4 M. Galanski, V. B. Arion, M. A. Jakupec and B. K. Keppler, *Curr. Pharm. Des.*, 2003, **9**, 2078–2089.
5 M. A. Jakupec, M. Galanski, V. B. Arion, C. G. Hartinger and B. K. Keppler, *Dalton Trans.*, 2008, 183–194.
6 P. Köpf-Maier, *Eur. J. Clin. Pharmacol.*, 1994, **47**, 1–16.
7 F. Kratz and M. T. Schutte, *Cancer J.*, 1998, **11**, 176–182.
8 I. Ott and R. Gust, *Arch. Pharm. Chem. Life Sci.*, 2007, **340**, 117–126.
9 S. H. van Rijt and P. J. Sadler, *Drug Discovery Today*, 2009, **14**, 1089–1097.
10 G. Xu, Y. B Cui, K. Cui and S. H. Gou, *Prog. Chem.*, 2006, **18**, 107–113.
11 F. Caruso and M. Rossi, *Mini-Rev. Med. Chem.*, 2004, **4**, 49–60.
12 F. Caruso, M. Rossi and C. Pettinari, *Expert Opin. Ther. Pat.*, 2001, **11**, 969–979.
13 C. V. Christodoulou, A. G. Eliopoulos, L. S. Young, L. Hodgkins, D. R. Ferry and D. J. Kerr, *Br. J. Cancer*, 1998, **77**, 2088–2097.
14 G. Kelter, N. J. Sweeney, K. Strohfeldt, H.-H. Fiebig and M. Tacke, *Anti-Cancer Drugs*, 2005, **16**, 1091–1098.
15 B. K. Keppler, C. Friesen, H. G. Moritz, H. Vongerichten and E. Vogel, *Struct. Bonding*, 1991, **78**, 97–127.
16 P. Köpf-Maier and H. Köpf, *Chem. Rev.*, 1987, **87**, 1137–1152.
17 P. Köpf-Maier and H. Köpf, *Struct. Bonding*, 1988, **70**, 103–185.
18 E. Melèndez, *Crit. Rev. Oncol. Hematol.*, 2002, **42**, 309–315.
19 K. Strohfeldt and M. Tacke, *Chem. Soc. Rev.*, 2008, **37**, 1174–1187.
20 F. Caruso, L. Massa, A. Gindulyte, C. Pettinari, F. Marchetti, R. Pettinari, M. Ricciutelli, J. Costamagna, J. C. Canales, J. Tanski and M. Rossi, *Eur. J. Inorg. Chem.*, 2003, 3221–3232.
21 J. H. Toney and T. J. Marks, *J. Am. Chem. Soc.*, 1985, **107**, 947–953.
22 D. Peri, S. Meker, C. M. Manna and E. Y. Tshuva, *Inorg. Chem.*, 2011, **50**, 1030–1038.
23 D. Peri, S. Meker, M. Shavit and E. Y. Tshuva, *Chem.–Eur. J.*, 2009, **15**, 2403–2415.
24 M. Shavit, D. Peri, C. M. Manna, J. S. Alexander and E. Y. Tshuva, *J. Am. Chem. Soc.*, 2007, **129**, 12098–12099.
25 E. Y. Tshuva and J. A. Ashenhurst, *Eur. J. Inorg. Chem.*, 2009, 2203–2218.
26 E. Y. Tshuva and D. Peri, *Coord. Chem. Rev.*, 2009, **253**, 2098–2115.
27 C. M. Manna, M. Shavit and E. Y. Tshuva, *J. Organomet. Chem.*, 2008, **693**, 3947–3950.
28 C. S. Higham, D. P. Dowling, J. L. Shaw, A. Cetin, C. J. Ziegler and J. R. Farrell, *Tetrahedron Lett.*, 2006, **47**, 4419–4423.
29 C. J. Whiteoak, G. J. P. Britovsek, V. C. Gibson and A. J. P. White, *Dalton Trans.*, 2009, 2337–2344.
30 P. Hormnirun, E. L. Marshall, V. C. Gibson, A. J. P. White and D. J. Williams, *J. Am. Chem. Soc.*, 2004, **126**, 2688–2689.
31 J. Balsells, P. J. Carroll and P. J. Walsh, *Inorg. Chem.*, 2001, **40**, 5568–5574.
32 A. J. Chmura, M. G. Davidson, M. D. Jones, M. D. Lunn, M. F. Mahon, A. F. Johnson, P. Khunkamchoo, S. L. Roberts and S. S. F. Wong, *Macromolecules*, 2006, **39**, 7250–7257.
33 S. Groysman, E. Sergeeva, I. Goldberg and M. Kol, *Eur. J. Inorg. Chem.*, 2005, 2480–2485.
34 A. Yeori, S. Groysman, I. Goldberg and M. Kol, *Inorg. Chem.*, 2005, **44**, 4466–4468.
35 A. Nielson and J. J. M. Waters, *Polyhedron*, 2010, **29**, 1715–1726.
36 Unpublished results: additional complexes of NH donors investigated in our laboratory also yielded dinuclear complexes as the main hydrolysis products.